into the melt, melt-depleted mantle should also have low $^{186}Os/^{188}Os$, unlike Meibom and Frei's samples.

Elevated $^{186}Os/^{188}Os$ accompanied by high $^{187}Os/^{188}Os$ has been reported in lavas from Siberia (*3*) and Hawaii (*4*). Oceanic basalts have been known for some time to have high $^{187}Os/^{188}Os$, and this was generally attributed to the presence of recycled crust in the mantle (*2*). (Crust is generated by melting of the mantle and will therefore have high Re/Os and Pt/Os.)

Brandon *et al.* (*4*) argued that the magnitude of variation in $^{186}Os/^{188}Os$ seen in Hawaiian lavas was too great to explain by mixing old crust back into the mantle. They attributed the result instead to the incorporation of a small amount of core material into the mantle before it departed from the core-mantle boundary and rose as a thermal plume beneath Hawaii. Based on what is known from iron meteorite analogs, crystallization of the inner core will leave the outer core with high Pt/Os and Re/Os. Because Os concentrations in the core are much higher than in the mantle, even a fraction of a percent of core material will noticeably alter the Os isotopic composition of the mantle.

Meibom and Frei's results indicate that, in their samples, core-mantle mixing and the formation of the Os-alloys must have occurred long ago, before the core's $^{187}Os/^{188}Os$ ratio grew to exceed that of the modern mantle. They further use the data to derive constraints on the partitioning behavior of Re, Pt, and Os during core crystallization and suggest that formation of the inner core must already have been well under way within 250 million years of Earth's formation.

This conclusion is of considerable interest because a solid inner core appears to be critical in establishing a dipole magnetic field by controlling convective circulation in the liquid outer core. Furthermore, early inner core formation implies rapid initial cooling of Earth. Given the present size of the still-liquid outer core, this limits subsequent heat loss from the core over Earth's history (unless the core has its own heat source via incorporation of radioactive elements like uranium and/or potassium, a possibility that is not widely accepted). The amount of heat transfer across the core-mantle boundary influences both the vigor of mantle convection and whether the mantle flow leaving the boundary is characterized by broad upwellings or narrow plumes. Elucidating the transfer of heat and material across the core-mantle boundary is thus of crucial importance for understanding the dynamics—and chemical consequences—of convection in the solid earth.

References

1. A. Meibom, R. Frei, *Science* **296**, 516 (2002).
2. S. B. Shirey, R. J. Walker, *Annu. Rev. Earth Planet. Sci.* **26**, 423 (1998).
3. R. J. Walker *et al.*, *Geochim. Cosmochim. Acta* **61**, 4799 (1997).
4. A. D. Brandon, R. J. Walker, J. W. Morgan, M. D. Norman, H. M. Prichard, *Science* **280**, 1570 (1998).

PERSPECTIVES: PHASE OF MATTER

The Elusive Liquid-Solid Interface

Erik Johnson

In macroscopic terms, the boundary between a liquid in contact with a solid surface is described by an interface energy that determines how the liquid wets or spreads out on the surface. If the interface energy is high, wetting is limited; if the interface energy is low, there is nearly complete wetting; in between, one talks about partial wetting. On a microscopic level, the interface is a two-dimensional surface with macroscopic dimensions along the contact surface, yet perpendicular to the surface, it is often considered as a discontinuity with infinitesimal thickness.

During the last couple of decades, however, it has become clear that the structure of the liquid-solid interface is more complex than anticipated. Experiments and computer simulations have shown that a degree of ordering progresses in layers from the solid surface over a few atomic distances into the liquid. On page 507 of this issue, Donnelly *et al.* (*1*) beautifully demonstrate this phenomenon for liquid xenon in contact with aluminum crystal facets. They report high-resolution transmission electron microscopy (TEM) of aluminum samples containing liquid xenon inclusions within faceted aluminum cavities. By viewing the samples with the aluminum facets in an edge-on orientation, they were able to look along the interface and obtain direct evidence for ordering parallel to the interface in the liquid xenon in the three layers nearest to the aluminum surface.

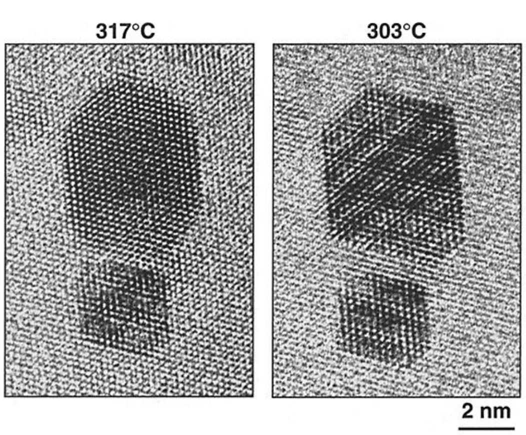

Solidification of a lead inclusion in aluminum. Solidification occurs at a lower temperature than the bulk melting point of 327°C. In the image on the left, taken at 317°C, the larger, somewhat rounded inclusion is still liquid, whereas it has solidified in the image on the right, taken at 303°C, and regained full faceting. The small inclusion is solid in both images. The lattice seen in the liquid inclusion is from the enclosing aluminium matrix, making it impossible to ascertain whether layer ordering exists in the liquid. The images obtained by Donnelly *et al.* (*1*) from xenon inclusions in aluminum are superior because in this particular case, the contrast from the aluminum matrix could be diminished by carefully selecting the orientation of the samples.

The authors used ion implantation to produce aluminum samples containing xenon inclusions a few nanometers in diameter. They exploited the property that a small particle—free or embedded—is confined under a pressure $P = 2\gamma/r$, where r is the radius of the particle and γ is the surface energy for a free particle or the interface energy for an embedded particle (*2*). The interface energy between xenon and aluminum is practically equal to the surface energy of aluminum of 1.2 J m^{-2} (*3*). For inclusions with $r < 2$ nm, it follows that P is in the Gigapascal range, high enough for xenon to be solid at room temperature. Somewhat larger inclusions will be under lower pressure and contain liquid xenon.

Solid noble gas inclusions in aluminum were first discovered by conventional TEM around 1984 (*4, 5*). Recently, Furuya and co-workers (*6, 7*) have produced beautiful atomic-resolution TEM images of solid xenon inclusions. Similar TEM studies have been carried out on solid lead inclusions embedded in aluminum (*8*). During heating experiments carried out in the TEM, it has been possible to follow the melting and solidification transitions of the lead inclusions in situ (see the figure) (*9*). However, no insights into

---

The author is at the Orsted Laboratory, Niels Bohr Institute, University of Copenhagen, Universitetsparken 5, DK-2100 Copenhagen O, Denmark. E-mail: johnson@fys.ku.dk

the structure of the liquid could be gained from these studies.

Experimental elucidation of the atomic structure of the liquid-solid interface is inherently difficult. Embedded between the liquid and the contacting surface, the interface is not easily accessible, and the amount of material contained in the interface is extremely small and limited to a few atomic layers. Lead is well suited to liquid surface and interface studies under ultrahigh-vacuum conditions, because it is easy to keep clean, and its vapor pressure is very low even at the melting point. It was used in the pioneering work by Frenken and van der Veen (*10*), who by means of medium-energy ion channeling showed that non-close-packed crystal facets of lead display disordering of the top few surface layers at temperatures well below the bulk melting point. Computer simulations (*11*) for aluminum confirmed the phenomenon of premelting, which is now accepted as a general property of non-close-packed surfaces. A degree of layer ordering is retained in the premelted material (*11*), providing a key to understanding the liquid-solid interface.

With the advent of x-ray synchrotron radiation facilities of extremely high brilliance, instruments have become available for studies of monolayers. These tools have been used to demonstrate lateral anisotropy in a monolayer of liquid lead on germanium (*12*) and layer ordering in the interface between liquid gallium and diamond (*13*). Recently, Reichert *et al.* (*14*) have shown distinct layer ordering in liquid lead on a silicon surface and demonstrated that the in-plane ordering has fivefold symmetry, representative for the building blocks used to describe liquid structures.

Atomic-resolution TEM instruments are not normally associated with studies of liquid-solid interfaces, with some notable exceptions. A few years ago, Howe (*15*) presented a well-designed TEM study that mimicked a liquid-solid interface. He studied the interface between amorphous $Pd_{80}Si_{20}$ and crystalline Pd_3Si, arguing that layer ordering in the amorphous phase may reflect an analogous ordering in the liquid-solid interface. Also using TEM, Sasaki and Saka (*16*) have shown how the solid alumina phase grows layer by layer from the liquid at the solid-liquid alumina interface. The work by Donnelly *et al.* (*1*) follows in this tradition, clearly demonstrating that very detailed information on structures in liquids can be achieved by TEM on carefully chosen systems.

The work by Donnelly *et al.* (*1*) sets a new standard for the use of TEM in the study of liquids in contact with solids. Together with the works by Howe (*15*) and Sasaki and Saka (*16*), it presents the TEM community with new challenges for designing and investigating liquid-solid interface systems and using TEM to obtain information that is otherwise only accessible by use of large-scale x-ray synchrotron facilities.

References

1. S. E. Donnelly *et al., Science* **296**, 507 (2002); published online 21 March 2002 (10.1126/science.1068521).
2. D. A. Porter, K. A. Easterling, *Phase Transformations in Metals and Alloys* (Chapman and Hall, London, 1992), p. 45.
3. A. R. Miedema, *Solid State Commun.* **39**, 1337 (1981).
4. A. vom Velde *et al., Phys. Rev. Lett.* **53**, 922 (1984).
5. C. Templier, R. J. Gaboriaud, H. Garem, *Mater. Sci. Eng.* **69**, 63 (1985).
6. N. Ishikawa *et al., Nucl. Instrum. Methods Phys. Res. B* **127/128**, 123 (1997).
7. C. W. Allen *et al., J. Electron. Microsc.* **48** (suppl.), 1025 (1999).
8. U. Dahmen, E. Johnson, S. Q. Xiao, A. Johansen, *MRS Bull.* **22** (no. 8), 49 (1997).
9. S. Q. Xiao *et al., J. Microsc.* **180**, 61 (1995).
10. J. W. M. Frenken, J. F. van der Veen, *Phys. Rev. Lett.* **54**, 134 (1985).
11. P. Stoltze, J. K. Nørskov, U. Landman, *Phys. Rev. Lett.* **61**, 440 (1988).
12. F. Grey *et al., Phys. Rev. B* **41**, 9519 (1990).
13. W. J. Huisman *et al., Nature* **390**, 379 (1997).
14. H. Reichert *et al., Nature* **408**, 839 (2000).
15. J. M. Howe, *Philos. Mag. A* **74**, 761 (1996).
16. K. Sasaki, H. Saka, *Mater. Res. Soc. Symp. Proc.* **466**, 185 (1997).

Published online 21 March 2002;
10.1126/science.1070400
Include this information when citing this paper.

PERSPECTIVES: COMPUTING

Successes and Challenges

John H. Reif

In the last few years, the idea of a molecular computer that could execute computational steps at the scale of a single molecule has moved from the realm of science fiction into that of scientific publications. Eight years ago, Adleman (*1*) demonstrated the first small-scale molecular computation. From this ground-breaking experiment sprang the rapidly evolving field of DNA computation, or biomolecular computing (*2*), which uses biotechnological techniques to do computation.

On page 499 of this issue, Braich *et al.* (*3*) report by far the largest scale demonstration to date of the capabilities of DNA computation. This landmark study proves that molecular computation is not a far-fetched possibility, but a quickly evolving discipline that may have major impact on more established disciplines such as biotechnology.

DNA provides a compact means of data storage and a degree of parallelism far beyond that of conventional silicon-based computers. In principle, more than 10^{21} bits of information are packed into each gram of dehydrated DNA. Routine recombinant DNA techniques for detection, amplification, and editing of DNA can be used for massively parallel molecular computation, because they simultaneously operate on each strand of DNA in a test tube. A single recombinant DNA operation can take up to 20 minutes or so, but the high degree of molecular parallelism still provides immense capabilities for efficient computation, because even routine experiments can involve between 10^{15} and 10^{17} strands of DNA in a small test tube. The rapid evolution of biotechnology and use of automation also provides increased scaling capabilities.

Braich *et al.* (*3*) use DNA computing to solve a satisfiability (SAT) problem—a combinatorial search problem where we are given an expression that defines a logical relationship between two or more items (a Boolean formula) and wish to find a truth assignment to the variables to satisfy the formula. As a very simple example, the Boolean formula "($\sim x_1$ or x_2 or x_3) and (x_1 or $\sim x_2$ or x_3) and (x_1 or x_2 or $\sim x_3$) and ($\sim x_1$ or $\sim x_2$ or $\sim x_3$)," where "~" denotes logical "not," has a truth assignment of all the variables to false. SAT is known to be a NP-hard problem, which computer scientists view as unlikely to have a fast solution on a conventional computer for large instances of the problem.

Recent progress on the SAT Problem with DNA computations may lead to unreasonable expectations. The use of DNA computation to solve very large combinatorial search problems such as SAT cannot be scaled up indefinitely. The number of distinct DNA strands generally grows exponentially with the size of the problem statement, and the molecular-scale data storage is eventually swamped by the numbers of DNA strands required for large problems. For the SAT Problem, the likely upper limit is 70 to 80 Boolean variables.

Nevertheless, moderately sized SAT problems have served as a useful test for DNA computation techniques. Generally, these methods involve the generation of a combinatorial library of synthetic DNA

The author is at the Computer Science Department, Duke University, Durham, NC 27708, USA. E-mail: reif@cs.duke.edu